Structural, Electronic, and Magnetic Properties Of Co n Cu m Nanoalloys (m + n = 12) from First Principles Calculations

ARTICLE *in* THE JOURNAL OF PHYSICAL CHEMISTRY A · AUGUST 2012

Impact Factor: 2.69 · DOI: 10.1021/jp3017997 · Source: PubMed

4 AUTHORS:

F. Aguilera-Granja
Universidad Autónoma de San Luis Potosí
150 PUBLICATIONS **1,369** CITATIONS
SEE PROFILE

M. Begoña Torres
Universidad de Burgos
30 PUBLICATIONS **268** CITATIONS
SEE PROFILE

Andrés Vega
Universidad de Valladolid
176 PUBLICATIONS **1,951** CITATIONS
SEE PROFILE

Carlos Balbás
Universidad de Valladolid
136 PUBLICATIONS **2,250** CITATIONS
SEE PROFILE

THE JOURNAL OF PHYSICAL CHEMISTRY A

Article

pubs.acs.org/JPCA

Structural, Electronic, and Magnetic Properties Of Co_nCu_m Nanoalloys ($m + n = 12$) from First Principles Calculations

F. Aguilera-Granja,[†] M. B. Torres,*[,‡] A. Vega, and L. C. Balbás[§]

[†]Instituto de Física, Universidad Autónoma de San Luis Potosí, San Luis Potosí, México

[‡]Departamento de Matemáticas y Computación, Universidad de Burgos, Spain

[§]Departamento de Física Teórica, Atómica y Óptica, Universidad de Valladolid, Spain

ABSTRACT: Using the generalized gradient approximation (GGA) to density functional theory (DFT), we compute the electronic structure and related magnetic properties of free-standing $Co_{12-x}Cu_x$ clusters (x = 0−12) with structures resulting from the optimization of those of the low-lying energy isomers of pure Co_{12} and Cu_{12} in which Co(Cu) were replaced by Cu(Co) atoms. Structural transitions for the lowest energy homotop are obtained as a function of the concentration, but in all cases, a clear surface segregation of Cu is found in the low concentration regime $x < 5$. The binding energy decreases monotonically when x increases. The dipole moment changes abruptly from 0.06 D for $x = 2$ to 0.59 D for $x = 3$ in coincidence with a structural change. The electronegativity of the lowest energy homotop exhibits minimum (maximum) value for $x = 11$ ($x = 9$). The $x = 5, 9$ clusters show local maxima of the hardness, of the excess energy, and of the second difference in energy, clear indicators of specially stable stoichiometries. The magnetic behavior of $Co_{12-x}Cu_x$ is a monotonous function of the Co concentration, decreasing by steps of $\geq 2\ \mu_B$ for every Co atom that is replaced by Cu, although for certain concentrations, different spin isomers, sometimes accompanied by structural transitions, are found close to the ground state. Ferromagnetic-like order is obtained as the ground state in all cases, contrary with the trend found in binary clusters of the same elements by other authors who predicted antiferromagnetic order. We analyze in detail the possible spin excitations in $Co_{12}Cu$ to demonstrate that local antiferromagnetic couplings can only exist as metastable spin states.

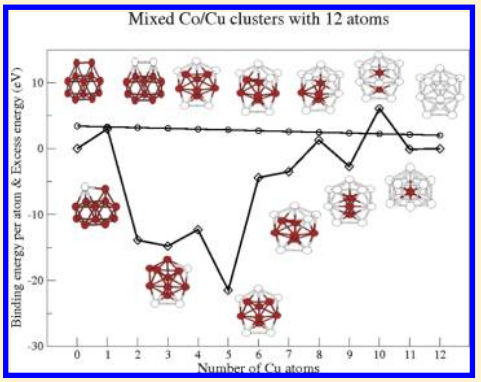

INTRODUCTION

The study of bimetallic clusters is interesting because their physical and chemical properties can be modified and eventually adjusted to desired ones by tuning not only the atomic order and size like in pure clusters but also their composition, atomic order, and size. In this work, we study the ionic and electronic structure of Co_nCu_m clusters with $n + m = 12$ and their main electronic properties. A motivation is the giant magneto-resistance (GMR) observed in Co clusters embedded in Cu matrix.[1] The factors controlling the GMR effect in granular materials are mainly the size distribution and the volume fraction of the ferromagnetic Co particles embedded in the nonferromagnetic matrix as well as the roughness of the interfaces.[2] Ferromagnetic behavior was observed in cobalt-rich bulk Cu_xCo_{100-x} systems (x = 20−100) at room temperature while the $Cu_{90}Co_{10}$ system showed paramagnetic behavior.[3] Just to mention another application, among many others, we cite the enhanced electrocatalytic activity of cobalt−copper nanostructures recently observed by Ahmed and co-workers.[4] The magnetism of Co nanoparticles suported on a Cu(111) surface was studied earlier by two of us.[5]

The structure of ground-state and low-lying energy isomers of Co_{12} and Cu_{12} seems to be well-established.[6] The properties of $Co_{18-m}Cu_m$ ($0 \leq m \leq 18$) were investigated by Wang and co-workers using a semiempirical nonrestricted Hartree−Fock model for a spd band.[8] They obtained a clear tendency of Cu to stay at the surface sites whereas Co prefers the volume. For the same concentrations shells are formed of equal atoms. A few selected configurations of Co_nCu_m with $n + m < 13$ were studied by Lu and co-workers,[9] particularly those with $n = 1$, $m = 1$, and $n = m + 1$. They obtained strong structural deformations and a tendency to segregation similar to that observed by Wang and co-workers.[8] However, the ground-state and low energy isomers structures of Co_n and Cu_n clusters with $n \leq 19$ recently reported by two of us[10,11] are different to those reported by Wang et al.[12] Concerning the electronic properties, Lu et al. predicted antiferromagnetic-like order with a concomitant low total spin for the ground state of these bimetallic clusters, even in the low Cu concentration limit like in $Co_{12}Cu$.

Considering that the structure of the Co_nCu_m nanoalloys plays a crucial role in their electronic and magnetic properties, in this work, we address the study of $Co_{12-x}Cu_x$ with different initial geometries. We start with the known structures of low-lying energy isomers of pure Co_{12} and Cu_{12} clusters,[10,11] that is,

Received: February 23, 2012
Revised: August 16, 2012

   dx.doi.org/10.1021/jp3017997 | J. Phys. Chem. A XXXX, XXX, XXX−XXX

(i) hexagonal compact planar (HCP), (ii) planar icosahedral like (ICO-P), (iii) icosahedral minus one apex atom (ICO-M), and (iv) a planar type based on the buckled biplanar (BBP) structure. Many $Co_{12-x}Cu_x$ structures constructed from these geometries, as explained in the Theoretical Method Section below, will be optimized in order to select the most stable homotop of a given stoichiometry. Our aim is to determine, by means of ab initio total energy calculations, the stability indicators (binding energy, excess energy, second difference in energy), the structural trends (deformation and segregation effects), and the main electronic properties (magnetic moment and magnetic order, ionization potential, electronic affinity, hardness) of $Co_{12-x}Cu_x$ nanoalloys as a function of their composition. In the next section, we describe our theoretical approach including the main details of the calculations and the strategy for searching the optimal structures. In the Results Section, we present and discuss the energetics, structural properties, and electronic properties. The last part of that section is devoted to show that the ground state of these bimetallic clusters has ferromagnetic-like order, contrary to what was proposed by Lu and co-workers.[9] In the Conclusions Section, a summary of the conclusions is given.

THEORETICAL METHOD

To investigate the structural and magnetic properties of Co_nCu_m clusters (with $n + m = 12$), we used the computational package SIESTA, described in detail in ref 13. This code use numerical pseudoatomic orbitals as basis sets to solve the single particle Kohn−Sham equations of density functional theory (DFT).[14] For the exchange and correlation potential, we used the Perdew−Burke−Ernzerhof form of the generalized gradient approximation (GGA).[15] The atomic cores were described by nonlocal norm-conserving Troullier−Martins pseudopotentials[16] factorized in the Kleinman−Bylander form.[17] The pseudopotentials for Co and Cu were generated using the valence configurations $4s^13d^7$ and $4s^13d^{10}$, respectively. The pseudopotential radii employed in our calculations were 2.00 au for the s, p, and d orbitals of Co, and 2.08, 2.30, and 2.08 a.u for the s, p, and d orbitals of Cu. We also included nonlinear core corrections, at a radius of 0.75 au for both elements, in order to account for the overlap between the valence states and the core electrons. Valence states were described using double-ζ doubly polarized basis sets. The clusters were placed in a box of size 20 × 20 × 20 Å^3. We consider only the Γ point when integrating over the Brillouin zone as usual for finite systems. The energy cutoff defining the real-space grid for the numerical calculations was 250 Ry. We considered an electronic temperature of 25 meV for smearing the electronic states and facilitate the convergence, carried out with a criterium of 10^{-3} for the density matrix. The cluster structures were fully relaxed without any geometrical or spin constrains using the conjugate gradient method[18] until the interatomic forces were smaller than 0.006 eV/Å. The same setup of SIESTA was employed in a previous study by two of us on the pure 13 atom transition metal clusters.[19]

The search of low-lying energy homotops of $Co_{12-x}Cu_x$ was conducted as follows. We started with those four low-lying energy isomers of pure Co_{12} and Cu_{12} that are represented in Figure 1. The HCP structure is the lowest energy Co_{12} isomer resulting from the Co_{13} ground state[19] after subtracting one Co atom. The BBP and ICO-M structures are the first and second isomers of Co_{12}, respectively, resulting after subtracting a Co atom from the first and second isomers of Co_{13}, respectively.

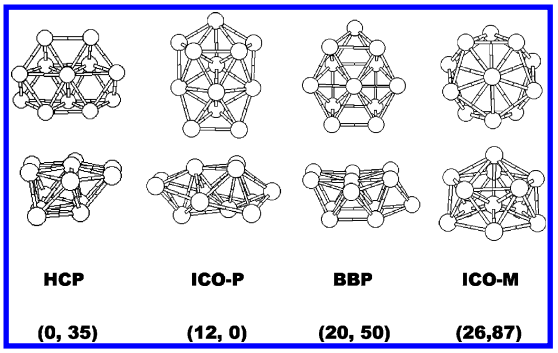

Figure 1. Top view (upper) and lateral view (down) of the initial cluster structures considered in this work. HCP = hexagonal compact; ICO-P = planar icosahedrom; BBP = buckled biplanar; ICO-M = icosahedral minus an (apex) atom. Below each structure is given in parentheses the total energy per atom, in meV, with respect to the lowest equilibrium energy of Co_{12} and Cu_{12}, respectively. For example, the ICO-M structure of Co_{12} (Cu_{12}) is 26 mev (87 meV) per atom above the Co_{12} (Cu_{12}) ground state energy. (color online).

The ICO-P structure is the ground-state isomer of Cu_{12} from ref 20, which results to be an isomer of Co_{12} with 12 meV higher energy than its ground-state HCP structure. The second step was to optimize the total energy of all possible $Co_{11}Cu$ initial configurations resulting from the substitution of a Co by a Cu atom in all the inequivalent sites for each one of the geometries shown in Figure 1. Then, we selected the three lowest energy homotops of these $Co_{11}Cu$ isomers for each one of the four initial geometries and substituted again a Co atom by a Cu atom in all the possible ways to select, after optimizing, again the three lower energy $Co_{10}Cu_2$ homotops for each one of the geometries shown in Figure 1. This procedure was repeated until we reached the equiatomic Co_6Cu_6 stoichiometry. The same procedure was pursued from the other side, that is, starting with the pure Cu_{12} isomers until converging with the previous series at the equiatomic stoichiometry. For each structural isomer/homotop, we did first a calculation in the free-spin mode. This usually provides, in the case of ferromagnetic-like clusters, the most stable spin isomer. We further checked this by performing additional calculations in the fix-spin mode for the adjacent total spin states, to ensure that the obtained spin state corresponded to the most stable spin configuration.

RESULTS

Figures 2−5 show the most stable $Co_{12-x}Cu_x$ homotops ($0 \le x \le 12$) with each of the structures HCP, ICO-P, BBP, and ICO-M shown in Figure 1, respectively. Figure 6 shows the collection of the overall most stable $Co_{12-x}Cu_x$ homotops ($0 \le x \le 12$) among those having any of these structures. We notice in Figure 1 that HCP (ICO-P) is the lowest energy homotop of the pure Co_{12} (Cu_{12}) cluster and that the four structures correspond to low-lying isomers of both pure Co_{12} and Cu_{12} within a window of less that 90 meV. We also note that mixing both elements does not produce noticeable deformations of the structures for any family. Noticeable structural deformations are expected in bimetallic clusters of atoms with markedly different atomic radii and/or markedly different atomic packing, which is not the case of the Co−Cu bimetallic clusters. In our case, the morphology is thus mainly dictated by the different energetic parameters of Co and Cu (binding energy, surface energy). Besides, the four families of structures are low-lying structural

dx.doi.org/10.1021/jp3017997 | J. Phys. Chem. A XXXX, XXX, XXX−XXX

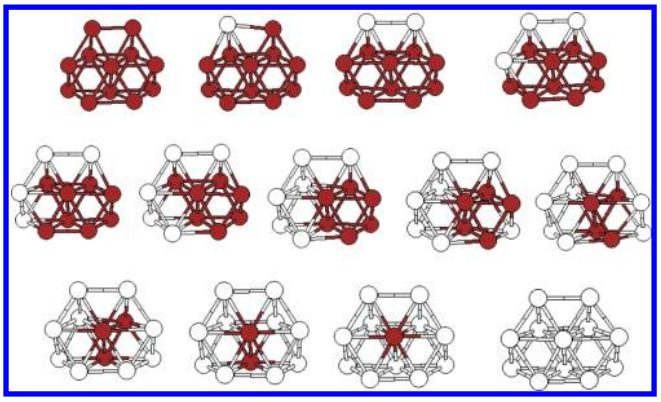

Figure 2. Geometry of the most stable $Co_{12-x}Cu_x$ clusters with HCP planarlike structure from $x = 0$ (upper left) to $x = 12$ (down right). (Color online).

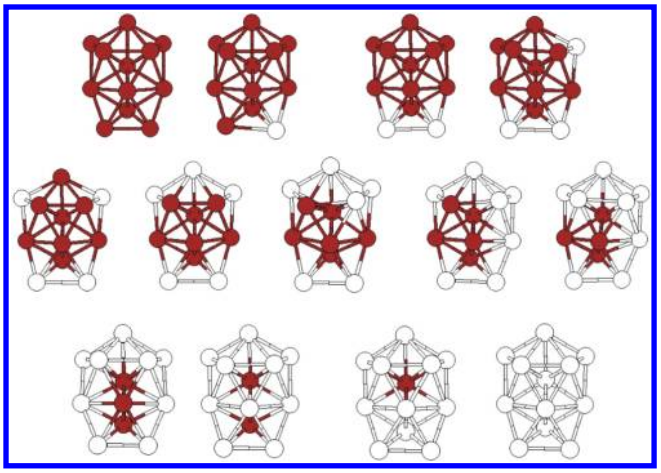

Figure 3. Geometry of the $Co_{12-x}Cu_x$ clusters with planar icosahedral ICO-P structure from $x = 0$ (upper left) to $x = 12$ (down right). (Color online).

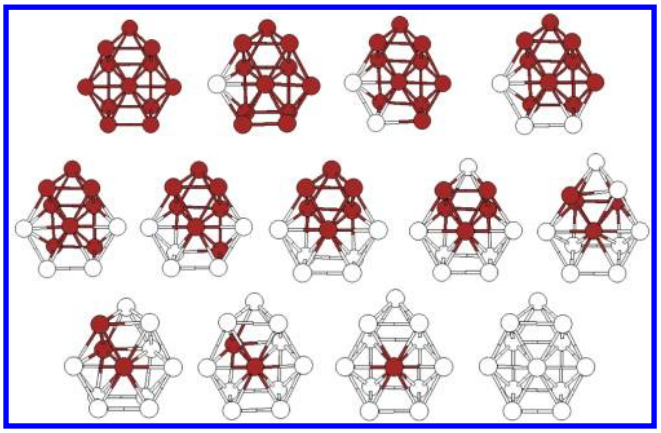

Figure 4. Geometry of the $Co_{12-x}Cu_x$ clusters with buckled biplanar BBP structure from $x = 0$ (upper left) to $x = 12$ (down right). (Color online).

isomers of both the pure clusters Co_{12} and Cu_{12}. Therefore, we did not expect noticeable structural deformations. In order to further confirm our assessment, we performed additional calculations for the clusters Co_6Cu_6 and Co_2Cu_{10} in their most stable configurations but inducing a random structural deformation with variations of about 15% in the coordinates in such a way that the input geometry had no symmetry at all. The

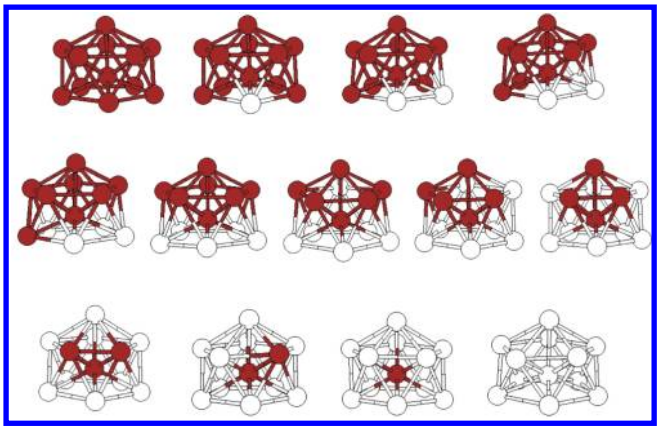

Figure 5. Geometry of the $Co_{12-x}Cu_x$ clusters with icosahedral minus an (apex) atom ICO-M structure from $x = 0$ (upper left) to $x = 12$ (down right). (Color online).

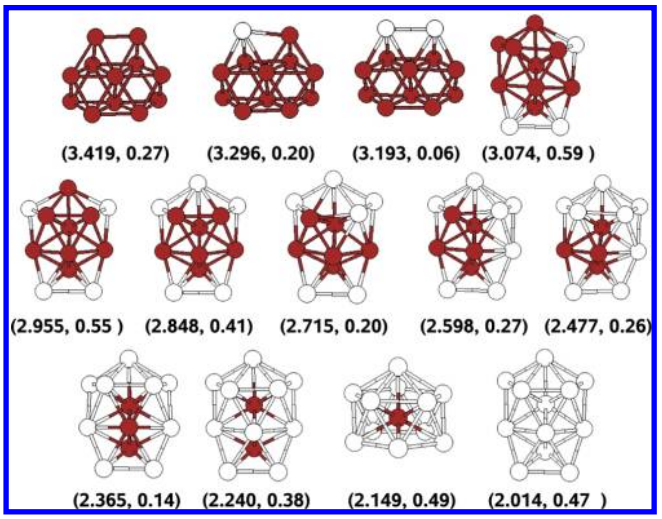

Figure 6. Geometry of the lowest energy $Co_{12-x}Cu_x$ isomer among those with structures as shown in Figure 1. Below are given the binding energy per atom, in eV, and the dipole moment, in Debye. (Color online).

goal was to check if a deformed variant of the putative ground-state symmetry was obtained after reoptimization or if the cluster evolved instead to the same putative ground state or to a different structural isomer belonging to another family of structures. The calculations have yielded the same putative ground state, which means that the local minima were well-captured and that the mixing of these two elements does not lead to strong structural deformations.

Tables 1−4 give several structural and electronic properties of the clusters represented in Figures 2−5, respectively.

The first column in these tables identifies the $Co_{12-x}Cu_x$ homotop by its x value. Those x values in bold character correspond to the overall lowest energy one. The second column gives the binding energy per atom, $E_b(Co_{12-x}Cu_x)$, defined as

$$E_b(Co_{12-x}Cu_x) = \frac{1}{12}[E(Co_{12-x}Cu_x) - (12 - x)E(Co) - xE(Cu)] \quad (1)$$

where $E(A)$ is the total energy of system A.

dx.doi.org/10.1021/jp3017997 | J. Phys. Chem. A XXXX, XXX, XXX−XXX

Table 1. Electronic and Geometrical Properties of $Co_{12-x}Cu_x$ Clusters for $0 \leq x \leq 12$ with HCP Geometry[a]

x	energy (eV/atom)	order (σ)	Co−Co (Å)	Cu−Cu (Å)	Co−Cu (Å)	distance (Å)	ionization (eV)	affinity (eV)
0	3.419	1.00 (0.00)	2.404 (32)	–	–	2.404	6.075	1.980
1	3.296	0.75 (4.00)	2.405 (28)	–	2.537 (4)	2.422	6.106	2.010
2	3.193	0.63 (4.00)	2.404 (25)	2.601 (1)	2.518 (6)	2.432	6.097	2.003
3	3.064	0.44 (4.34)	2.395 (21)	2.552 (2)	2.533 (9)	2.444	6.147	1.937
4	2.936	0.31 (4.25)	2.395 (18)	2.552 (3)	2.531 (11)	2.457	6.193	2.034
5	2.824	0.16 (4.40)	2.393 (12)	2.548 (5)	2.538(12)	2.472	6.129	2.104
6	2.706	0.25 (4.67)	2.378 (12)	2.543 (8)	2.551 (12)	2.484	6.058	1.986
7	2.576	0.00 (4.57)	2.362 (8)	2.544 (8)	2.550 (16)	2.501	6.187	2.004
8	2.454	−0.06 (4.63)	2.345 (5)	2.533 (10)	2.558 (17)	2.517	6.349	2.099
9	2.340	0.00 (4.67)	2.336 (3)	2.550 (13)	2.548 (16)	2.529	6.281	2.020
10	2.223	0.13 (4.80)	2.292 (1)	2.548 (17)	2.536 (14)	2.534	6.225	2.029
11	2.101	0.44 (5.00)	–	2.553 (23)	2.553(9)	2.545	6.030	2.005
12	1.979	1.00 (5.34)	–	2.566 (32)	–	2.566	6.516	2.012

[a]First column specifies the number of Cu atoms, x. Bold face numbers correspond to the lowest energy isomer among those with HCP, ICO-P, ICO-M, and BBP initial symmetry. The successive columns give the following: the binding energy per atom, E_b (see eq 1); the order parameter σ (see eq 2), with the coordination number of Cu in parentheses; the average bond length of Co−Co bonds (fourth column), Cu−Cu bonds (fifth column), and Co−Cu bonds (sixth column), with the corresponding number of bonds in parentheses. The total average bond distance is given in the seventh column. The eighth and ninth columns give the ionization potential and electron affinity, respectively.

Table 2. Same as Table 1 for $Co_{12-x}Cu_x$ Clusters with ICO-P Geometry

no. Cu	energy (eV/atom)	order (σ)	Co−Co (Å)	Cu−Cu (Å)	Co−Cu (Å)	distance (Å)	ionization (eV)	affinity (eV)
0	3.407	1.00 (0.00)	2.427 (34)	–	–	2.427	6.103	2.039
1	3.292	0.76 (4.00)	2.423 (30)	–	2.569 (4)	2.440	6.092	2.017
2	3.188	0.65 (4.00)	2.434 (27)	2.699 (1)	2.521 (6)	2.457	6.104	2.034
3	3.074	0.41 (4.00)	2.427 (23)	2.701 (1)	2.553 (10)	2.472	6.119	1.985
4	2.955	0.18 (4.00)	2.434 (19)	2.703 (1)	2.546 (14)	2.488	6.093	1.955
5	2.848	0.12 (4.20)	2.419 (16)	2.600 (3)	2.555 (15)	2.495	6.111	1.853
6	2.715	0.00 (4.50)	2.399 (12)	2.594 (5)	2.553 (17)	2.505	6.064	1.986
7	2.598	0.00 (4.71)	2.403 (9)	2.607 (8)	2.540 (17)	2.520	6.194	2.027
8	2.477	0.00 (4.88)	2.390 (6)	2.592 (11)	2.548 (17)	2.534	6.130	1.989
9	2.365	0.00 (5.00)	2.347 (3)	2.596 (14)	2.535 (17)	2.543	6.303	2.046
10	2.240	0.24 (5.30)	2.328 (1)	2.571 (20)	2.544 (13)	2.553	6.158	1.956
11	2.137	0.47 (5.36)	–	2.572 (25)	2.530 (9)	2.561	6.404	1.948
12	2.014	1.00 (5.67)	–	2.565 (34)	–	2.565	6.549	1.935

Table 3. Same as Table 1 for $Co_{12-x}Cu_x$ Clusters with BBP Geometry

no. Cu	energy (eV/atom)	order (σ)	Co−Co (Å)	Cu−Cu (Å)	Co−Cu (Å)	distance (Å)	ionization (eV)	affinity (eV)
0	3.399	1.00 (0.00)	2.408 (32)	–	–	2.408	6.085	1.988
1	3.279	0.69 (5.00)	2.399 (27)	–	2.548(5)	2.422	6.032	2.033
2	3.161	0.56 (4.50)	2.405 (24)	2.565 (1)	2.536 (7)	2.439	6.065	2.094
3	3.046	0.44 (4.34)	2.401 (21)	2.535 (2)	2.541 (9)	2.449	6.607	2.098
4	2.930	0.25 (4.50)	2.389 (17)	2.545 (3)	2.556 (12)	2.466	6.058	2.038
5	2.807	0.19 (4.60)	2.388 (14)	2.541 (5)	2.543 (13)	2.475	6.093	2.202
6	2.705	0.25 (4.67)	2.388 (12)	2.534 (8)	2.542 (12)	2.482	6.114	1.937
7	2.579	0.00 (4.57)	2.368 (8)	2.547 (8)	2.543 (16)	2.500	6.065	2.092
8	2.452	−0.06 (4.63)	2.342 (5)	2.557 (10)	2.541 (17)	2.515	6.123	2.035
9	2.326	0.06 (4.78)	2.346 (3)	2.544 (14)	2.548 (15)	2.527	6.141	2.060
10	2.218	0.13 (4.80)	2.286 (1)	2.555 (17)	2.543 (14)	2.541	6.155	1.977
11	2.112	0.38 (4.91)	–	2.537 (22)	2.542 (10)	2.538	6.114	1.968
12	1.964	1.00 (5.33)	–	2.557 (32)	–	2.557	6.313	1.960

Figure 6 gives the binding energy and electric dipole moment of the lowest energy $Co_{12-x}Cu_x$ clusters. We see that the binding energy per atom decreases in absolute value monotonically from $x = 0$ to $x = 12$. Instead, the dipole moment changes abruptly from 0.06 D for $x = 2$ to 0.59 D for $x = 3$, in coincidence with a structural transition from the HCP to the ICO-P geometry (see Figure 6). Since these are the structures of the pure Co_{12} and Cu_{12} clusters, respectively, a structural transition of this kind is expected to take place. However, Co_1Cu_{11} is found to have a ICO-M symmetry instead of any of the other two, which is unexpected and provides evidence of the fact that the ground-state geometry of a bimetallic cluster can be different from that of the pure clusters of the same size. In this respect, care was taken in our structural search by considering not only the lowest energy structures of the pure clusters but also several low-lying isomers. In the low x zone of

dx.doi.org/10.1021/jp3017997 | J. Phys. Chem. A XXXX, XXX, XXX−XXX

Table 4. Same as Table 1 for $Co_{12-x}Cu_x$ Clusters with ICO-M Geometry[a]

no. Cu	energy (eV/atom)	order (σ)	Co−Co (Å)	Cu−Cu (Å)	Co−Cu (Å)	distance (Å)	ionization (eV)	affinity (eV)
0	3.393 (24)	1.00 (0.00)	2.449 (36)	–	–	2.449	5.921	2.049
1	3.267 (22)	0.72 (5.00)	2.442 (31)	–	2.592 (5)	2.463	5.914	1.941
2	3.146 (20)	0.56 (5.00)	2.437 (27)	2.725 (1)	2.568(8)	2.474	5.914	1.956
3	3.027 (18)	0.39 (5.00)	2.433 (23)	2.727 (2)	2.575 (11)	2.493	5.863	2.020
4	2.914 (16)	0.23 (5.00)	2.418 (19)	2.754 (3)	2.549 (14)	2.497	5.874	1.951
5	2.804 (14)	0.17 (5.00)	2.426 (16)	2.726 (5)	2.533 (15)	2.512	5.854	1.866
6	2.684 (10)	0.06 (5.16)	2.384 (12)	2.628 (7)	2.561 (17)	2.515	5.763	1.898
7	2.560 (8)	0.06 (5.28)	2.385 (9)	2.633 (10)	2.536 (17)	2.525	5.661	1.917
8	2.445 (6)	0.06 (5.37)	2.385 (6)	2.623 (13)	2.527 (17)	2.538	5.653	1.881
9	2.326 (6)	0.06 (5.44)	2.346 (3)	2.544 (14)	2.548 (15)	2.527	5.743	1.906
10	2.234 (4)	−0.11 (5.50)	2.468 (1)	2.515 (15)	2.600 (20)	2.561	5.890	1.814
11	2.149 (2)	0.39 (5.54)	–	2.597 (25)	2.484 (11)	2.562	5.872	1.785
12	1.927 (0)	1.00 (6.00)	–	2.600 (36)	–	2.600	6.118	1.968

[a]The second column also gives (in parentheses) the total magnetic moment because, contrary to other geometries, its value decreases non-monotonically when the content of Cu increases: from $x = 5$ to $x = 6$, the step is 4 μ_B instead of 2 μ_B, and from $x = 8$ to $x = 9$, there is no change of magnetic moment.

Figure 6, we see that Cu substitutes Co atoms with low coordination whereas in the high x zone Co substitutes Cu with high coordination.

In order to analyze qualitatively the chemical order (segregation or mixing) of our $Co_{12-x}Cu_x$ nanoalloys as a function of the relative composition, in the third column of Tables 1−4 is given the order parameter, σ, which is analogous to the one introduced by Ducastelle[21] for the study of bulklike binary alloy systems. In our case, it is defined as

$$\sigma = \frac{N_{Cu-Cu} + N_{Co-Co} - N_{Cu-Co}}{N_{Cu-Cu} + N_{Co-Co} + N_{Co-Cu}} \quad (2)$$

where N_{A-B} is the number of nearest-neighbors bonds between A and B atoms. σ is positive when phase separation or segregation takes place, negative when mixing happens, and ≈0 when transition from segregation to mixing phase appears in the system ($\sigma \approx 0$ identifies a disordered phase, although for finite systems this phase is very similar to the mixing one (see the sketch in the inset of Figure 7). In bulklike binary systems, the parameter σ allows making of a clear distinction between disorder ($\sigma \approx 0$) and mixing (small negative values of σ), but it allows also characterizing other types of ordered phases like the layered-like phase (large negative values of σ). Figure 7 shows the parameter σ as a function of x for the most stable $Co_{12-x}Cu_x$ homotop. The $\sigma(x)$ value for those clusters with the HCP geometry of pure Co_{12} and an average of $\sigma(x)$ for the four geometries in Figure 1 are also given for comparison. We see that segregation occurs in most cases.

The third column of Tables 1−4 gives in parentheses the average coordination number of Cu atoms. The average coordination of Cu_{12} with geometry HCP, ICO-P, BBP, and ICO-M results to be 5.34, 5.67, 5.34, and 6.00, respectively. Considering the lowest energy isomer of $Co_{12-x}Cu_x$ clusters (see Figure 6), we observe that Cu tends to be in the cluster surface (low coordinated sites) and Co tends to occupy the more coordinated sites. This trend correlates with the smaller binding energy and surface energy of Cu compared to Co in pure bulk and semi-infinite systems.[22] The smaller atomic radius of Co as compared with Cu also favors its being located at the inner part of the cluster.

This trend correlates with the smaller (larger) surface energy (atomic radius) of Cu compared to Co in pure bulk systems.[22]

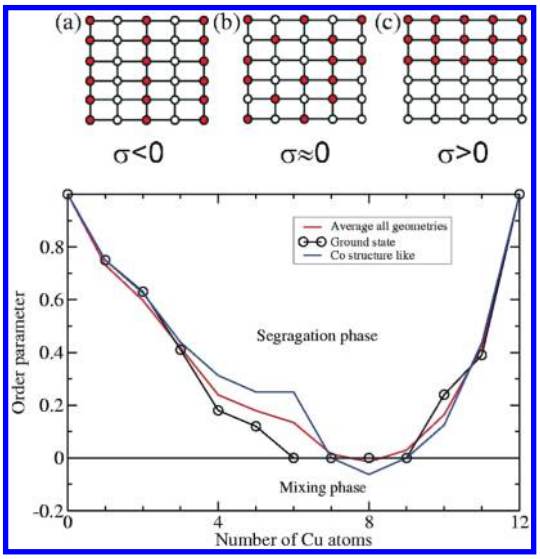

Figure 7. In the upper panels, a schematic graphical meaning of the order parameter σ of eq 2 is given: (a) $\sigma < 0$ indicates an alloy phase, (b) $\sigma \approx 0$ corresponds to a disordered phase, and (c) $\sigma > 0$ indicates segregation phase. The lower part shows the average σ values for $Co_{12-x}Cu_x$ as a function of the number of Cu atoms. Black circles represent the ground-state values, the blue line connects the σ values for those clusters with the HCP structure, and the red line connects the average value for the HCP, ICO-P, BBP, and ICO-M structures given in Figures 2−5. (Color online).

The fourth, fifth, sixth, and seventh columns of Tables 1−4 give the average bond lengths of Co−Co, Cu−Cu, Co−Cu, and the average atom−atom distances, respectively. The last increases monotonically from 2.40 to 2.56 Å, which correlates with the monotonous decreasing trend of the binding energy per particle.

The eight and ninth columns of Tables 1−4 give the ionization potential (IP) and electron affinity (EA), respectively. Panel (a) of Figure 8 shows the electronegativity (χ = (IP + EA)/2) and hardness (η = (IP − EA)/2) for the more stable $Co_{12-x}Cu_x$ homotop as a function of the number of Cu atoms. The electronegativity shows a pronounced minimum (maximum) for $x = 11$ ($x = 9$). Notice that, for $x = 11$, the Co atom is inside the cluster and that, for $x = 9$, all the Cu atoms are in the surface (see Figure 6). Thus, experiments about the

dx.doi.org/10.1021/jp3017997 | J. Phys. Chem. A XXXX, XXX, XXX−XXX

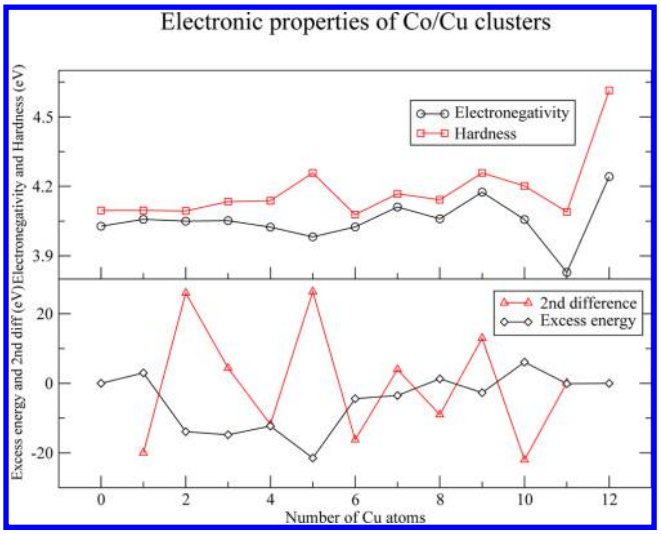

Figure 8. Lowest energy $Co_{12-x}Cu_x$ clusters with $0 \leq x \leq 12$ are given. (Upper panel) electronegativity (black circles) and hardness (red squares); (Lower panel) excess binding energy, E_{excess} and second energy difference, E_2, (triangles) defined in eqs 2 and 3, respectively. (Color online).

adsorption rate of H_2, F_2, O_2, and other small molecules on $Co_{12-x}Cu_x$ clusters are expected to show strong distinct features for $x = 9$, 11 stoichiometries. On the other hand, the hardness, which is related to the HOMO−LUMO gap of the cluster, shows local peaks for $x = 5$, 9 clusters (apart of pure Cu_{12}).

In order to further assess the relative stability of particular stoichiometries, it is also useful to discuss the excess energy, defined for these clusters as

$$E_{excess}(Co_{12-x}Cu_x) = E_b(Co_{12-x}Cu_x) - (12 - x)\frac{E_b(Co_{12})}{12} - x\frac{E_b(Cu_{12})}{12} \quad (3)$$

where $E_b(Z_N) = N \times E(Z) - E(Z_N)$ is the binding energy of a cluster Z_N and $E(Z_N)$ is its total energy. This quantity E_{excess} was used by previous authors[6,7] to determine the relative stability of several phases of binary nanoalloys. A negative value of E_{excess} indicates in general that mixing is favorable. Another interesting quantity in this same context is the second energy difference, defined as

$$E_2(Co_{12-x}Cu_x) = E_b(Co_{12-x-1}Cu_{x+1}) + E_b(Cu_{12-x+1}Cu_{x-1}) - 2 \times E_b(Co_{12-x}Cu_x) \quad (4)$$

Clusters with high relative stability correspond to peaks in $E_2(Co_{12-x}Cu_x)$. Panel (b) of Figure 8 shows $E_{excess}(Co_{12-x}Cu_x)$ and $E_2(Co_{12-x}Cu_x)$. We see that both quantities show marked peaks for $x = 5$, 9 in coincidence with the local peaks of the hardness, that is, signaling these stoichiometries as specially stable ones. Notice that the several magnitudes represented in Figure 8 show odd−even electronic effects only in the interval $3 \leq x \leq 10$ where no structural change appears.

The magnetic moment of the lowest energy $Co_{12-x}Cu_x$ clusters decreases regularly in steps of 2 μ_B as going from $x = 0$ (24 μ_B) to $x = 12$ (0 μ_B). This trend is observed also for each one of the cluster series with the structures shown in Figure 1, except for the ICO-M series. In that case, the magnetic moment (given in parentheses in the second column of Table 4) for $x = 6$, 7, or 8, is 10 μ_B, 8 μ_B, or 6 μ_B, respectively. Thus, in the interval $6 \leq x \leq 8$, where no special features appear in Figure 8, we found two structural−magnetic homotops, with ICO-M and ICO-P geometries, respectively. The corresponding binding energies differ by ≈32 meV per atom, and their total magnetic moment differ by 2 μ_B.

Ferromagnetic-like order is obtained as the ground state of $Co_{12-x}Cu_x$ clusters, contrary with the trend found in binary clusters of the same elements by other authors who predicted antiferromagnetic order.[9] In the following paragraphs, we analyze in detail the possible spin excitations in $Co_{12}Cu$ to demonstrate that local antiferromagnetic couplings can only exist as metastable spin states.

Lu and co-workers have investigated Co/Cu and Co/Pt bimetallic clusters of 13 atoms[9] in the framework of DFT using the Dmol3 code[23] with the GGA aproximation of Wang and Perdew (PW91) for exchange and correlation.[24] They have determined the putative ground-state structures by optimizing, at the DFT level, the lowest energy structures previously obtained using a genetic algorithm with a Gupta-like many-body potential. Their predicted ground states were icosahedrons. We will come to this point later. As it regards the magnetic properties, these authors predicted a quite unexpected behavior in the case of Co/Cu clusters. Thus, they predicted an antiferromagnetic arrangement, even in the limit of the Co rich phase, that is, $Co_{12}Cu$, which leads to a weak total spin magnetic moment. For instance, in the case of $Co_{12}Cu$, they predicted a total moment of only 1 μ_B, together with a decreasing behavior of the binding energy if the total moment increases to 3, 5, and 7 μ_B. Since this trend is in principle unexpected for clusters formed by late transition-metal elements (whose bulks are ferromagnetic), we wanted to perform a more systematic study of the $Co_{12}Cu$ cluster with icosahedral structure.

In order to have a sufficient benchmark of the results, we have used two different codes: the SIESTA code (that employs pseudopotentials to describe the core interactions and pseudoatomic orbital in the basis, as detailed in the previous section) and the VASP[25] code. The plane-wave code VASP, solves the spin-polarized Kohn−Sham equations within the projector-augmented wave method.[26] This allows a considerable efficiency in terms of computational time, and it is in principle a better approximation than the pseudopotential one used in SIESTA. With both codes, we optimize the atomic positions using the conjugate gradients algorithm.

First of all, we calculated the spin isomer with a total spin of 1 (we can fix the total spin in our calculations). This state, corresponding to a doublet, exists due to the formation of antiparallel magnetic couplings between Co atoms, but it has a considerable lower binding energy than the state with total moment of 23 μ_B and parallel couplings, that is, the ferromagnetic-like configuration with essentially 2 μ_B per Co atom. The difference of total binding energy between both self-consistent magnetic solutions obtained with VASP/PBE is 1.27 eV. This is at odds with the predictions of Lu et al.,[9] although they do not report data for the ferromagnetic solution. In order to check if our result is due to a different treatment of exchange and correlation effects, we also calculated both solutions using the PW91 functional[24] (the same used by Lu et al.[9]). The result is quite the same; PW91 gives 1.20 eV smaller total binding energy for the antiferromagnetic state than the ferromagnetic state. Similar results are obtained using SIESTA/PBE. In that

dx.doi.org/10.1021/jp3017997 | J. Phys. Chem. A XXXX, XXX, XXX−XXX

case, the difference in energy amounts to 1.08 eV. We note that the optimized geometrical structure is also similar in both cases and also similar to the one obtained using SIESTA/PBE, that is, the icosahedral symmetry is preserved.

The next step was to perform calculations for other low-spin isomers to try to find a clear picture of the possible antiferromagnetic excitations of this cluster. Once verified that SIESTA/PBE, VASP/PBE, and VASP/PW91 gave essentially the same results, we selected SIESTA/PBE for these calculations due to the lower computational requirements as compared with VAPS and for the sake of comparison with the rest of results reported in the present work. In Figure 9, we

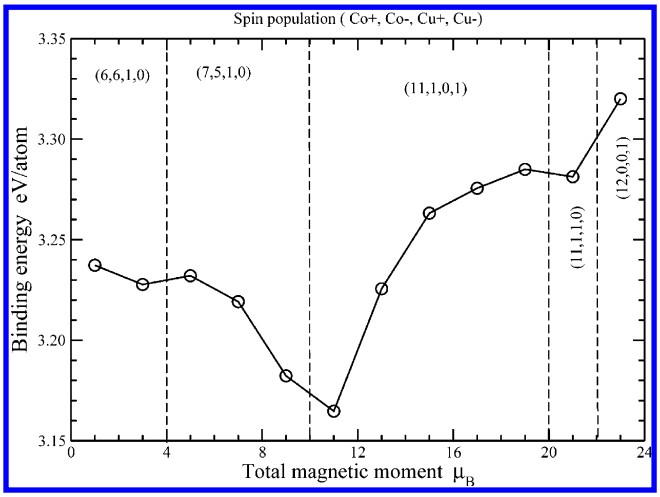

Figure 9. Binding energy per atom (eV) of $Co_{12}Cu$ cluster as a function of the total magnetic moment. The number of atoms (Co↑, Co↓, Cu↑, Cu↓) with spin up (↑) and spin down (↓) of Co and Cu are given for different regions separated by vertical dashed lines. (Color online).

plot the binding energy as a function of the total magnetic moment of $Co_{12}Cu$. The curve shows that all antiferromagnetic states are magnetic excitations of the ground state with 23 μ_B and ferromagnetic-like order. However, it is interesting to note a non-monotonic behavior as a function of the total spin, with a minimum of the binding energy obtained for a total spin of 11 μ_B. This means that some antiferromagnetic excitations with rather compensated moments and correspondingly weak total magnetization result more accessible than others with larger total moment. This unexpected trend was found by Lu et al.[9] for the four spin isomers with lowest total moment. We stress that anyway the ground state is ferromagnetic and that the lowest energy spin isomers are those with a large total moment and a small degree of antiferromagnetic order (only few atoms are found with their moments coupled antiparallel).

Some comments are also pertinent in regard to the lowest energy structural configuration proposed by Lu et al.[9] SIESTA calculations predict a biplanar structure as the lowest energy one for Co_{13} among those tested in a previous work,[11] including the icosahedrons. This biplanar structure has been also predicted for Co_{13} in a recent work by Dong and Gong[27] using VASP and results from the one found in the present work for the 12 atom clusters plus an additional atom in. The difference in binding energy with respect to the icosahedral structure is about 1 eV. We guess that this biplanar structure resulted in probably a high-energy isomer in the genetic algorithm used by Lu et al. based on the Gupta potential, as it is well-known that Gupta tends to favor spherical structures, in particular icosahedral ones. Nevertheless, our calculations give the same ground-state ferromagnetic configuration for this structure and for the icosahedral one.

CONCLUSIONS

We have calculated the structural, electronic, and magnetic properties of $Co_{12-x}Cu_x$ clusters with $0 \leq x \leq 12$ starting with HCP, ICO-P, ICO-M, and BBP initial structures of pure Co and Cu isomers. An exhaustive search of the lowest energy homotop for each stoichiometry is done by means of a ladder procedure. We find a transition from the HCP structure in the rich Co concentration region to ICO-P structure as the Cu concentration increases, although $Co_{11}Cu_1$ is found to have a ICO-M symmetry instead of any of the other two. This provides evidence of the fact that the ground-state geometry of a bimetallic cluster can be different from that of the pure clusters of the same size and that the exhaustive structural search was pertinent. The chemical order of these nanoalloys is marked by the tendency of the Co atoms to occupy high coordination sites and the tendency of Cu atoms to be placed in the low coordination surface sites. This trend, which leads to segregation in most cases, is consistent with the smaller (higher) surface energy (radius) of Cu compared to Co bulk phases.

The binding energy (average interatomic distance) monotonically decreases (increases) as x increases. The dipole moment changes abruptly from $x = 2$ to $x = 3$ in coincidence with the structural change from HCP to ICO-P. The electronegativity of the lowest energy homotop exhibits minimum (maximum) value for $x = 11$ ($x = 9$). For $x = 5, 9$, we have found local maxima of the hardness (HOMO−LUMO gap) and of the second difference in energy, which are clear indicators of specially stable stoichiometries.

Magnetic moments show a monotonic decrease as the concentration of Cu increases. For $6 \leq x \leq 8$, two structural−magnetic isomers (ICO-P and ICO-M) are found with ≈32 meV binding energy per atom difference. Ferromagnetic-like order is obtained as the ground state in all cases, contrary with the trend found in binary clusters of the same elements by other authors who predicted antiferromagnetic order even in the low Cu concentration limit. Our detailed study of the possible spin excitations in $Co_{12}Cu$ demonstrates however that local antiferromagnetic couplings can only exist as metastable spin states.

AUTHOR INFORMATION

Corresponding Author

*E-mail: begonia@ubu.es.

Notes

The authors declare no competing financial interest.

ACKNOWLEDGMENTS

We acknowledge the support of the Spanish Ministerio de Ciencia e Innovación, the European Regional Development Fund, and Junta de Castilla y León (grant nos. FIS2011-22957 and VA104A11-2). F.A-G acknowledges the financial support from PROMEP-SEPCA230, CONACyT 162651 and to the Ministerio de Educación, Cultura y Deporte, Ref. SAB2011-0024, Spain. We also acknowledge J. Limón for the computational support.

REFERENCES

(1) Baibich, M. N.; Broto, J. M.; Fert, A.; Nguyen Van Dau, F.; Petroff, F.; Etienne, P.; Greuzet, G.; Friedrich, A.; Chazelas, J. *Phys. Rev. Lett.* **1988**, *61*, 2472−2475. Binasch, G.; Grünberg, P.; Saurenbach, F.; Zinn, W. *Phys. Rev. B* **1989**, *39*, 4828−4830.

(2) Yang, G. Y.; Zhu, J.; Wang, W. D.; Zhang, Z.; Zhu, F. W. *Mater. Res. Bull.* **2000**, *35*, 875−885.

(3) Fan, X.; Mashimo, T.; Huang, X.; Kagayama, T.; Chiba, A.; Koyama, K.; Motokawa, M. *Phys. Rev. B* **2004**, *69*, 094432−1−094432−6.

(4) Ahmed, J.; Ganguly, A.; Saha, S.; Gupta, G.; Trinh, P.; Mugweru, A. M.; Lofland, S. E.; Ramanujachary, K. V.; Ganguli, A. K. *J. Phys. Chem. C* **2011**, *115*, 14526−14533.

(5) Izquierdo, J.; Vega, A.; Balbás, L. C. *Phys. Rev. B* **1997**, *55*, 445−451.

(6) Ferrando, R.; Jellinek, J.; Johnston, R. L. *Chem. Rev.* **2008**, *108*, 845−910.

(7) Paz-Borbon, L. O.; Gupta, A.; Johnston, R. L. *J. Mater. Chem.* **2008**, *18*, 4154−4164.

(8) Wang, J.; Wang, G.; Chen, X.; Lu, W.; Zhao, J. *Phys. Rev. B* **2002**, *66*, 014419−1−014419−5.

(9) Lu, Q. L.; Zhu, L. Z.; Ma, L.; Wang, G. H. *Chem. Phys. Lett.* **2005**, *407*, 176−179.

(10) Aguilera-Granja, F.; Vega, A. *Phys. Rev. B* **2009**, *79*, 144423−1−144423−2.

(11) Guzman-Ramírez, G.; Aguilera-Granja, F.; Robles, J. *Eur. Phys. J. D* **2010**, *57*, 335−342.

(12) Wang, B. L.; Chen, X.-S.; Chen, G.-B.; Wang, G.-H.; Zhao, J.-J. *Surf. Rev. Lett.* **2004**, *11*, 15−20.

(13) Soler, J. M.; Artacho, E.; Gale, J. D.; García, A.; Junquera, J.; Ordejon, P.; Sánchez-Portal, D. *J. Phys.: Condens. Matter* **2002**, *14*, 2745−2779.

(14) Hohemberg, P.; Kohn, W. *Phys. Rev. B* **1964**, *136*, 864−871. Kohn, W.; Sham, L. *Phys. Rev. B* **1965**, *145*, 561−567.

(15) Perdew, J. P.; Burke, K.; Ernzerhof, M. *Phys. Rev. Lett.* **1996**, *77*, 3865−3868.

(16) Troullier, N.; Martins, J. L. *Phys. Rev. B* **1991**, *43*, 1993−2006.

(17) Kleinman, L.; Bilander, D. M. *Phys. Rev. Lett.* **1982**, *48*, 1425−1428.

(18) Press, W. H.; Teukolsky, S. A.; Vetterling, W. T.; Flannery, B. P. *Numerical Recipes in Fortran*, 2nd ed.; Cambridge University Press: Cambridge, U.K., 1992.

(19) Aguilera-Granja, F.; García-Fuente, A.; Vega, A. *Phys. Rev. B* **2008**, *78*, 134425−1−134425−9.

(20) Fernández, E. M.; Soler, J. M.; Garzón, I. L.; Balbás, L. C. *Phys. Rev. B* **2004**, *70*, 165403−1−165403−14.

(21) Ducastelle, F. *Order and Phase Stability in Alloys*; de Boer, F. R., Petiffor, D. G., Eds.; North Holland: Amsterdam, The Netherlands, 1991.

(22) Vitos, L.; Ruban, A. V.; Skriver, H. L; Kollár, J. *Surf. Sci.* **1998**, *411*, 186−202.

(23) Accelrys.com

(24) Wang, Y.; Perdew, J. P. *Phys. Rev. B* **1991**, *43*, 8911−8916.

(25) Kresse, G.; Furthmüller, J. *Phys. Rev. B* **1996**, *54*, 11169−11186.

(26) Kresse, G.; Joubert, D. *Phys. Rev. B* **1999**, *59*, 1758−1775.

(27) Dong, C. D.; Gong, X. G. *Phys. Rev. B* **2008**, *78*, 020409(R).